Localization and RNAi-driven inhibition of a *Brugia malayi* encoded Interleukin-5 Receptor Binding protein

Rojelio Mejia[1], Sasisekhar Bennuru[1], Yelena Oksov[2] Sara Lustigman[2], Gnanasekar Munirathinam[3,] Ramaswamy Kalyanasundaram[3], Thomas B. Nutman[1*]

[1]Laboratory of Parasitic Diseases, National Institute of Allergy and Infectious Diseases, Bethesda, Maryland, USA. [2]Lindsay F. Kimball Research Institute, New York Blood Center, New York, NY, and [3]Department of Biomedical Sciences, College of Medicine, University of Illinois, Rockford, IL, USA.

Running title: *Brugia malayi* RNAi in L3

Corresponding author: Thomas B. Nutman tnutman@niaid.nih.gov

Keywords: *Brugia malayi*, RNAi, Host-parasite defense, Interleukin 5

Abstract

A molecule termed BmIL5Rbp (aka Bm8757) was identified from *Brugia malayi* filarial worms and found to competitively inhibit human IL-5 binding to its human receptor. After the expression and purification of a recombinant BmIL5Rbp and generation of BmIL5Rbp-specific rabbit antibody, we localized the molecule on *B. malayi* worms through immunohistochemistry and immunoelectron microscopy. RNA interference was used to inhibit BmIL5Rbp mRNA and protein production. BmIL5Rbp was shown to localize to the cuticle of *Brugia malayi* and to be released in their excretory/secretory products. RNAi inhibited BmIL5Rbp mRNA production by 33% and reduced the surface protein expression by ~50% and suppressed the release of BmIL5Rbp in the excretory/secretory products. RNAi has been used successfully to knock down the mRNA and protein expression of BmIL5Rbp in the early larval stages of *B. malayi* and provided a proof-of-principle for the local inhibition of the human IL5 receptor. These findings provide evidence that a parasite encoded IL5R antagonist could be utilized therapeutically.

Introduction

Filarial parasites are vector-borne nematodes that are responsible for >200 million infections, the most pathogenic of which are caused by *Wuchereria bancrofti, Brugia malayi* (two of the causative agents of lymphatic filariasis), *Onchocerca volvulus* (the causative agent of onchocerciasis or “river blindness”) and *Loa loa* (the causative agent of loiasis or “the Africa eyeworm”). Infection occurs when third-stage larvae (L3) are introduced into the skin, after which they migrate through the dermis into either deep or superficial lymphatics, where they continue their development. With the identification of innate lymphoid cells (ILC) (1) and tissue-resident eosinophils in the skin (2) and the fat associated subcutaneous tissue, and the fact that the filarial L3s can evade these crucial innate cell populations to establish infection suggests that there must be a common mechanism used by these skin-transiting parasites to establish infection in humans. This lack of response is believed to be due to the parasite's evasive immune mechanisms, especially the third-stage larvae (3).

Several helminth-encoded cytokine and chemokine mimics have been identified, largely through *in silico* analyses of genomic information. These include migration inhibitory factor (4-6) and TGF-β (7-9). A number of additional studies have used other methods to identify parasite-encoded molecules that are either agonists or antagonists of host-derived cytokine. Indeed, we identified in 2004, using a *B. malayi* L3 phage display library (10) a parasite-produced molecule called BmIL5Rbp (subsequent genome annotation Bm8757).

To understand the precise localization of this molecule in the *B. malayi* L3 and explore the feasibility of using L3s that fail to express this molecule for *in vivo* assessment/functional capabilities in relevant animal models, we used immunostaining and confocal microscopy to demonstrate the location and expression of BmIL5Rb. Using the RNAi approach on adults and microfilariae of *B. malayi* (11-14), we demonstrate its utility in L3s so that its role could be elucidated at the host-parasite interface.

Results

BmIL5Rbp is located on the surface of the worm and in the excretory-secretory products.

Using immunostaining to localize BmIL5Rbp on various stages of *B. malayi*, it can be seen that BmIL5Rbp was found to be expressed on the surface of the worm using electron microscopy (Figure 1) and laser confocal microscopy of the adult male, female, and L3 (Figure 2). As seen, BmIL5Rbp (red) is only demonstrated in the stacked images on the parasite surfaces. Interestingly, the protein is found dispersed throughout the worm's cuticle. No BmIL5Rbp was seen internal to the cuticle even when using fragmented or transected worms (data not shown).

Silencing BmIL5Rbp mRNA in L3 worms

To undertake the silencing of the BmIL5Rbp in L3s, we soaked L3 worms for two days in dsRNAi constructs for BmIL5Rbp or BmCPL (control) and examined the mRNA expression of the BmIL5Rbp. As shown in Figure 3A, BmIL5Rbp mRNA expression was diminished significantly compared to the BmCPL inhibited worms (33.1% vs. 4.89%, p = 0.0007) (Figure 3A). Approximately 85% of worms survived in both groups. Supernatants from live worms used in these RNAi cultured showed that the BmIL5Rbp protein content from these silenced worms showed levels of BmIL5Rbp (Figure 3B) that were 50% of the control worms (GM 205 pg/ml for the control siRNA construct and GM 105 pg for the siBmIL5Rbp group (P=0.034).

Detection and quantification of surface and excretory/secretory BmIL5Rbp

There was a 54% decrease in surface protein expression between the two groups of worms, as shown by the confocal images in Figure 4A. Quantification (Figure 4B) of fluorescence at the surface of the worms (Imaris) showed a similar reduction induced by siBmIL5Rbp (Figure 4B- 2.125 Intensity Sum/Voxels compared to 1.146 Intensity Sum/Voxels (p = 0.0025).

E/S products from worms silenced for BmIL5Rbp (or worms silenced for a control gene) showed decreased BmILRbp protein by 23% (Figure 4B).

Discussion

Lymphatic filarial parasites are notorious for their ability to manipulate host immune responses. In the present study, we show that one such mechanism

includes interfering with the function of host-derived IL-5. Here we characterize and localize the BmIL5Rbp produced by the third stage infective larvae of *B. malayi*, a secreted molecule that can bind to soluble human IL-5 receptor alpha and block the binding of human IL-5 to this receptor. Thus, BmIL5Rbp, a protein produced by *B. malayi,* appears to be a novel host-immunomodulatory molecule, acting as an IL5 antagonist.

The ability of a nematode-derived protein to alter the human host immune response is a unique evolutionary response that likely helps the worm to establish a foothold. We describe a nematode-produced protein found on the worm's surface (Figures 1, 2) and in its excretory/secretory product (Figures 3, 4).

B. malayi, along with all of the pathogenic filariae, induce a robust eosinophil response, particularly in the acute phase of infection (19, 20) related to the tissue migration L3 and L4 larvae of filarial nematodes (21-23). Our data suggest that these parasites secrete a molecule that antagonizes the activity of human IL-5, a cytokine found both early in infection and within days of anthelmintic chemotherapy (24-26).

The localization of BmIL5Rbp to the worm’s surface appears to be directly on (and within) the cuticle. Its location gives it accessibility to directly tissue-dwelling host cells bearing the IL5R (eosinophils, basophils, mast cells). It suggests that there may be a physiologic role for this molecule at the host tissue level. Since eosinophil worm killing is contact or localized dependent action (27), then the immediate areas, including the tissue, around the worm’s surface will

have higher concentrations of BmIL5Rbp, leading possibly to a loss of eosinophil survival at the site of inflammation/tissue damage.

The use of RNAi to selectively inhibit BmIL5Rbp helps to provide proof of principle that the worm produces a protein to inhibit the binding of human IL5 to its receptor. The RNAi-treated worms produced specifically less BmIL5Rbp that had less inhibition *in vitro*. With the advent of CRISPR-CAS9 in genomic splicing (28), the ability to knock out this gene now is a possibility (29-31). However, for the filarial nematodes, RNAi remains the most useful method of gene silencing (11, 12, 14, 17, 32-34).

Conclusion

While this study shows that it is feasible to silence the BmIL5Rb expression, *in vivo* experiments will be required to demonstrate the importance of this molecule (13). Our study provides a framework for utilizing these parasite-encoded cytokine antagonists for mechanistic and/or host-directed therapy studies that should, in turn, provide new insights into specific host-parasite interactions.

Methods

Electron microscopy and immunogold staining

The native BmIL5Rbp was identified in thin sections of *B. malayi* L3 by immuno-electron microscopy. The larvae were fixed with 4% paraformaldehyde/0.15% glutaraldehyde in 0.1 m sodium cacodylate buffer for 1 hour and embedded in LR White medium as previously described (15). Thin sections (70 nm) were then

blocked with 2% BSA and incubated with primary antibody (rabbit anti-rBmIL5) or control serum (pre-immunization bleed of the same rabbit) overnight at 4°C. Following washes in PBS containing 0.1% BSA and 0.01% Tween-20, grids were incubated with gold-labeled goat anti-mouse IgG (Fc) at 1:20 dilution (Amersham Pharmacia Biotech, Little Chalfont, United Kingdom) for 1 hour at room temperature, washed, counterstained in 5% uranyl acetate solution and observed using a Philips 410 electron microscope (Figure 1).

Immunostaining of L3 worms

L3 worms were fixed with a final concentration of 2% paraformaldehyde overnight at 4°C. Worms were washed three times with blocking buffer: 1% bovine serum albumin, 0.5% Triton X-100, 0.1% sodium azide, phosphate-buffered saline (PBS). The worms were soaked in 10 mMol sodium citrate (in blocking buffer) at 70°C for 60 minutes, washed three times in PBS, and soaked in blocking buffer overnight at 4°C. The worms were washed three times in PBS and then soaked in rabbit anti-BmIL5Rbp (1:10 in blocking buffer) for three days at 4°C. After washing three times in blocking buffer for 30 minutes, the worms were incubated with 1:500 dilution of goat anti-rabbit IgG Alexa Fluor 594 (Thermo Fisher Scientific, Waltham, MA) in blocking buffer for three days at 4°C. Phalloidin Alexa Fluor 488 (Thermo Fisher Scientific) in methanol (200 units/mL) was added and incubated overnight at 4°C. The worms were then washed three times with moderate shaking at 4°C for three hours each. Individual worms were collected and set with a mounting solution (Hardset VectaShield Vector H-1400,

Vector Laboratories, Burlingame, CA) overnight a 4°C. All worms were visualized using a confocal microscope, Leica SP5 X-WLL (Mannheim, Germany). Dapi stain was detected at 460 nm, Phalloidin at 520 nm, Alexa Fluor 594 at 620 nm with excitation at 595 nm at 15% laser power, a smart gain of 838, offset -0.3%.

Synthesis of siRNA constructs for BmIL5Rbp

Primers and probes for the gene sequence of BmIL5Rbp were designed using siRNA Target Designer-Version 1.6, Promega (Madison, WI) that used proprietary algorithms to select the optimal primer/probe sequences.

Forward 5'AAA AAG GGA ATT AGT TGT TG3'

Reverse 5'ATA CTA ACA AAC TTC TGC AAA TT3'

Plasmid DNA for BmIL5Rbp was generated and transformed to recombinant protein using TOP 10 *E. coli* competent cells (AMP resistant) (Thermo Fisher Scientific, Waltham, Ma). RNA PCR was performed using T7, T3 primers. Single-stranded RNA was annealed per-protocol (Agilent Technologies, Santa Clara, CA) with a final product of double-stranded RNA (dsRNA). DsRNA was concentrated using microcentrifugation filters and the final product was resuspended in PBS.

RNAi of *Brugia malayi* L3 worms

The L3 worms were cultured, as described previously (16). Double-stranded BmIL5Rbp (dsBmIL5Rbp) RNA was introduced to L3 worms by soaking, in which 20 L3 worms were soaked in 100 µL of dsBmIL5Rbp (500

µg/mL) in L3 media (16) for two days at 37°C. The media was removed, and 100 µL TRIzol® (Thermo Fisher Scientific) was added to the L3's and quickly frozen. The L3 larvae went through three freeze-thaw cycles and homogenated for five minutes at room temperature with Qiagen shredders (Qiagen, Venlo, Netherlands), washing with 100 µl TRIzol® (Thermo Fisher Scientific) three times. The macerated larvae were centrifuged at 12,000 g for one minute at 4°C between each wash. A total of 20 µL chloroform was then added to the shredded larvae and shaken vigorously for 15 seconds. The mixture was then centrifuged for 15 minutes at 12,000 g at 4°C. The aqueous phase was retained, and equal volumes of isopropanol were added. The aqueous phase mixture was centrifuged at 16,000 g for 15 minutes at 4°C. The pellet was washed with 70% ethanol then centrifuged at 16,000 g for 5 minutes at 4°C. The pellet was air-dried for 20 minutes, then re-suspended with 10 µL TE buffer (Thermo Fisher Scientific). Reverse transcription PCR was performed using standard techniques to the final volume of 100 µL. An internal control siRNA for *Brugia malayi* cathepsin L intron (BmCPL) (17) was created using the above protocol and was used to show specific inhibition of BmIL5Rbp using a SYBR Green real-time PCR (Applied Biosystems) per manufacturer specifications.

Primers for BmCPL (14).

Forward: 5' GAC AAA GAT TAC AAA CAG GGC3'

Reverse: 5' TGA TTG GGC AGT CGA AGT C3'

Real-time PCR quantification of BmIL5Rbp

Real-time PCR with final volumes of 20 µL, 1 µL of the probe (FAM-5'AAG CAA GCA TTG ATT TCT3'-MGBNFQ), 2 µL of template, 10 µL Taqman™ fast mix (Applied Biosystems, Foster City, CA), forward/reverse primers 1 µL each, 5 µl of dH_2O. Primers for BmIL5Rbp were selected upstream of the siRNA selection using the following primers:

Forward: 5'AAA ATG ATG GAA GCA GCA GAA ACT G3'

Reverse: 5'TAC AGG AAT ACA TCA TGC TCA CAA GT3'

All reactions were performed on an ABI 7900HT Fast Real-Time PCR System (Applied Biosystems). All primers and probes were purchased from Applied Biosystems. The PCR conditions were 95°C for 1 min 1 x cycle; 95°C for 25 s, 55°C for 20 s, 72°C for 1 min 35x cycles; 72°C for 10 min 1x cycle.

For standard comparison, housekeeping control Bm-tub primers were used with SYBR Green real-time PCR (Applied Biosystems) per manufacturer specifications (14).

Primers for Bm-tub (17)

Forward: 5'ATA TGT GCC ACG AGC AGT C3'

Reverse: 5'CGG ATA CTC CTC ACG AAT TT3'

Penetration of dsBmIL5Rbp in live *Brugia malayi*

DsBmIL5Rbp was Cy3 labeled using the CyDye™Post-Labelling Reactive Dye Pack (GE, Piscataway, NJ) per manufacturer's instructions. A total of 5 µL dsBmIL5Rbp (2000 µg/mL) was added to 100 mMol sodium bicarbonate and mixed with Cy3 in 20 µL DMSO stirred in the dark for 90 minutes at room

temperature. Then 15 µL of 4M hydroxylamine was added and mixed for 15 minutes in the dark at room temperature. Next, the mixture was precipitated with 5 µL of 5M sodium chloride for 60 minutes at 20°C. The solution was centrifuged at 16,000 g for 15 minutes at 4°C. Then to the supernatant, 175 µL of 70% cold ethanol was added, then centrifuged 16,000 g for 5 minutes at 4°C. Next, the supernatant was removed, and the pellet air-dried for 10 minutes in the dark and solubilized in 100 µL in L3 media (16). A total of 20 live L3 worms were soaked in the dsBmIL5Rbp media overnight. The worms were then fixed and mounted at the above methods. Also, 20 other worms were used in non-CY3 L3 media as a control group

Quantifying surface BmIL5Rbp on L3 worms using confocal microscopy.

Using the above RNAi methods, approximately 60 worms were exposed to BmIL5Rbp RNAi constructs. These were mounted along with appropriate control worms. Using a laser confocal microscope, capturing several 0.5mm stack images were obtained of entire worms. The intensity was calculated by using sum/voxels in Imaris (South Windsor, CT). Voxels are the total number of pixels at a specific wavelength.

Quantification of excretory/secretory BmIL5Rbp in L3 worms

BmIL5Rbp was measured using an immune dot blot. Briefly, nitrocellulose paper (Schleicher and Schuell (Keene, NH). was trimmed to fit a 96-well manifold. The paper was activated in methanol for three minutes and then washed for 1 min in

distilled water. The paper was dried, and 50 µL of rBmIL5Rbp (baculovirus derived) in various dilutions, duplicates were placed in wells with 50 µL of supernatants from RNAi and control worms. The plate was incubated at 37°C for one hour. The plate was dried, and the membrane was placed in a blocking buffer (5% milk, 5% rabbit serum, 5% goat serum) overnight at 4°C with gently tilting action. The membranes were incubated at room temperature in primary antibody Rabbit anti-BmIL5Rbp 1:100 dilution in 5% milk solution. The membrane was washed three times with 0.5% Tween 20 (Sigma-Aldrich, St. Louis, MO) in PBS solution for 5 min each cycle. Then a secondary antibody Goat anti-Rabbit Horseradish peroxidase (HRP) (Thermo Fisher Scientific) 1:1000 dilution in 5% milk was added for a 1-hour incubation at room temperature. The membrane was washed three times with 0.5% Tween and PBS solution for 5 minutes each cycle. For the ELISA developing step, a SuperSignal West Pico Chemiluminescent Substrate kit (Thermo Fisher Scientific) was used on the membrane as per the manufacturer's instructions. Luminescence was detected using Kodak X-OMAT film (Rochester, NY) and exposed for 10 minutes, then quantitated using BmIL5Rbp standard curves.

Measurement of decrease inhibition of human IL5 to its receptor *in vitro* using RNAi worms

A total of 50 µL/well of recombinant human IL5-Receptor alpha (R&D Systems, Minneapolis, MN) final concentration of (4 µg/mL) was plated using coating buffer (18) on Immulon 4 plates (Thermo Fischer Scientific) overnight at 4°C. The plates

were then washed with (0.2% Tween 20 in PBS) 6 times. A total of 100 µL of ELISA blocking buffer (0.05 Tween 20, 5% bovine serum albumin, PBS) was added for 1 hour at 37°C, with subsequent washing as above. Afterward, 25 µL of biotinylated recombinant human IL5 (rhIL5) protein (50 µg/mL) (R&D Systems) was added at 1:50 in PBS. Biotinylated rhIL5 was produced using the Biotin-X-NHS system (Merck, Darmstadt, Germany). A total of 25 µL of rhIL5 (100 µg/mL) was immediately added for a final concentration of 50 µg/mL and incubated at 37°C for one hour. The plate was washed as above, and 50 µL of streptavidin (Thermo Fisher Scientific) was added and incubated at 37°C for one hour. The plate was washed for a final time as above. The plate was developed with pNPP phosphatase substrate (Sigma, St. Louis, MO) per the manufacturer's instructions for 30 min at room temperature. Plates were read at 405 nm in an ELISA reader (SpectraMax Plus; Molecular Devices, Sunnyvale, CA). In determining the optimal concentration for Biotinylated rhIL5, a separate set of experiments was done with 2-fold dilutions using the above methods. Results showed that a 1:100 final concentration of biotinylated rhIL5 was the optimal concentration (data not shown).

Statistics and calculations

All statistical analysis was performed using Prism version 5.0d (GraphPad, La Jolla, CA). Comparisons were analyzed using the Mann-Whitney test, and P values < 0.05 were considered significant. RNAi results were shown as the percent reduction compared to a standard housekeeping control gene (Bm-tub)

as previously described (17). In summary, the control group value was set as the maximum amount with the RNAi-treated worms reported as a relative reduction compared to the internal control group (BmCPL). Calculation of intensity sum/voxels was completed with Imaris Software (Zurich, Switzerland).

References

1. Artis D, Spits H. 2015. The biology of innate lymphoid cells. Nature 517:293-301.
2. Cheng LE, Sullivan BM, Retana LE, Allen CD, Liang HE, Locksley RM. 2015. IgE-activated basophils regulate eosinophil tissue entry by modulating endothelial function. J Exp Med 212:513-24.
3. Cotton RN, McDonald-Fleming R, Boyd A, Spates K, Nutman TB, Tolouei Semnani R. 2015. Brugia malayi infective larvae fail to activate Langerhans cells and dermal dendritic cells in human skin. Parasite Immunol 37:79-91.
4. Wang Y, Lu M, Wang S, Ehsan M, Yan R, Song X, Xu L, Li X. 2017. Characterization of a secreted macrophage migration inhibitory factor homologue of the parasitic nematode Haemonchus Contortus acting at the parasite-host cell interface. Oncotarget 8:40052-40064.
5. Filbey KJ, Varyani F, Harcus Y, Hewitson JP, Smyth DJ, McSorley HJ, Ivens A, Nylen S, Rottenberg M, Loser S, Maizels RM. 2019. Macrophage Migration Inhibitory Factor (MIF) Is Essential for Type 2 Effector Cell Immunity to an Intestinal Helminth Parasite. Front Immunol 10:2375.
6. Chauhan N, Sharma R, Hoti SL. 2015. Identification and biochemical characterization of macrophage migration inhibitory factor-2 (MIF-2) homologue of human lymphatic filarial parasite, Wuchereria bancrofti. Acta Trop 142:71-8.
7. Gomez-Escobar N, Gregory WF, Maizels RM. 2000. Identification of tgh-2, a filarial nematode homolog of Caenorhabditis elegans daf-7 and human transforming growth factor beta, expressed in microfilarial and adult stages of Brugia malayi. Infect Immun 68:6402-10.
8. White MPJ, McManus CM, Maizels RM. 2020. Regulatory T-cells in helminth infection: induction, function and therapeutic potential. Immunology 160:248-260.

343 9. Johnston CJC, Smyth DJ, Kodali RB, White MPJ, Harcus Y, Filbey KJ, Hewitson
344 JP, Hinck CS, Ivens A, Kemter AM, Kildemoes AO, Le Bihan T, Soares DC,
345 Anderton SM, Brenn T, Wigmore SJ, Woodcock HV, Chambers RC, Hinck AP,
346 McSorley HJ, Maizels RM. 2017. A structurally distinct TGF-beta mimic from
347 an intestinal helminth parasite potently induces regulatory T cells. Nat
348 Commun 8:1741.
349 10. Gnanasekar M, Rao KV, He YX, Mishra PK, Nutman TB, Kaliraj P, Ramaswamy
350 K. 2004. Novel phage display-based subtractive screening to identify vaccine
351 candidates of Brugia malayi. Infect Immun 72:4707-15.
352 11. Singh M, Singh PK, Misra-Bhattacharya S. 2012. RNAi mediated silencing of
353 ATPase RNA helicase gene in adult filarial parasite Brugia malayi impairs in
354 vitro microfilaria release and adult parasite viability. J Biotechnol 157:351-8.
355 12. Landmann F, Foster JM, Slatko BE, Sullivan W. 2012. Efficient in vitro RNA
356 interference and immunofluorescence-based phenotype analysis in a human
357 parasitic nematode, Brugia malayi. Parasit Vectors 5:16.
358 13. Kushwaha S, Singh PK, Shahab M, Pathak M, Bhattacharya SM. 2012. In vitro
359 silencing of Brugia malayi trehalose-6-phosphate phosphatase impairs
360 embryogenesis and in vivo development of infective larvae in jirds. PLoS Negl
361 Trop Dis 6:e1770.
362 14. Aboobaker AA, Blaxter ML. 2003. Use of RNA interference to investigate gene
363 function in the human filarial nematode parasite Brugia malayi. Mol Biochem
364 Parasitol 129:41-51.
365 15. Zheng HJ, Tao ZH, Zhang XH, Piessens WF. 1989. [Further study on in vitro
366 culture of third-stage larvae of Wuchereria bancrofti and Brugia malayi].
367 Zhongguo Ji Sheng Chong Xue Yu Ji Sheng Chong Bing Za Zhi 7:276-9.
368 16. Bennuru S, Semnani R, Meng Z, Ribeiro JM, Veenstra TD, Nutman TB. 2009.
369 Brugia malayi excreted/secreted proteins at the host/parasite interface:
370 stage- and gender-specific proteomic profiling. PLoS Negl Trop Dis 3:e410.
371 17. Ford L, Zhang J, Liu J, Hashmi S, Fuhrman JA, Oksov Y, Lustigman S. 2009.
372 Functional analysis of the cathepsin-like cysteine protease genes in adult
373 Brugia malayi using RNA interference. PLoS Negl Trop Dis 3:e377.
374 18. Ravi V, King TP, Andersen JF, Nutman TB, Neva FA. 2005. Strongyloides
375 stercoralis recombinant NIE antigen shares epitope with recombinant Ves v
376 5 and Pol a 5 allergens of insects. Am J Trop Med Hyg 72:549-53.
377 19. Gebreselassie NG, Moorhead AR, Fabre V, Gagliardo LF, Lee NA, Lee JJ,
378 Appleton JA. 2012. Eosinophils preserve parasitic nematode larvae by
379 regulating local immunity. J Immunol 188:417-25.
380 20. Specht S, Saeftel M, Arndt M, Endl E, Dubben B, Lee NA, Lee JJ, Hoerauf A.
381 2006. Lack of eosinophil peroxidase or major basic protein impairs defense
382 against murine filarial infection. Infect Immun 74:5236-43.
383 21. Patnode ML, Bando JK, Krummel MF, Locksley RM, Rosen SD. 2014.
384 Leukotriene B4 amplifies eosinophil accumulation in response to nematodes.
385 J Exp Med 211:1281-8.
386 22. Faccioli LH, Mokwa VF, Silva CL, Rocha GM, Araujo JI, Nahori MA, Vargaftig
387 BB. 1996. IL-5 drives eosinophils from bone marrow to blood and tissues in a

388 guinea-pig model of visceral larva migrans syndrome. Mediators Inflamm
389 5:24-31.
390 23. Chitkara RK, Krishna G. 2006. Parasitic pulmonary eosinophilia. Semin Respir
391 Crit Care Med 27:171-84.
392 24. Limaye AP, Abrams JS, Silver JE, Ottesen EA, Nutman TB. 1990. Regulation of
393 parasite-induced eosinophilia: selectively increased interleukin 5 production
394 in helminth-infected patients. J Exp Med 172:399-402.
395 25. Cooper PJ, Chico ME, Sandoval C, Nutman TB. 2004. Atopic phenotype is an
396 important determinant of immunoglobulin E-mediated inflammation and
397 expression of T helper cell type 2 cytokines to ascaris antigens in children
398 exposed to ascariasis. J Infect Dis 190:1338-46.
399 26. Klion AD, Law MA, Noel P, Kim YJ, Haverty TP, Nutman TB. 2004. Safety and
400 efficacy of the monoclonal anti-interleukin-5 antibody SCH55700 in the
401 treatment of patients with hypereosinophilic syndrome. Blood 103:2939-41.
402 27. Cadman ET, Thysse KA, Bearder S, Cheung AY, Johnston AC, Lee JJ, Lawrence
403 RA. 2014. Eosinophils are important for protection, immunoregulation and
404 pathology during infection with nematode microfilariae. PLoS Pathog
405 10:e1003988.
406 28. Ghorbal M, Gorman M, Macpherson CR, Martins RM, Scherf A, Lopez-Rubio JJ.
407 2014. Genome editing in the human malaria parasite Plasmodium falciparum
408 using the CRISPR-Cas9 system. Nat Biotechnol 32:819-21.
409 29. You H, Mayer JU, Johnston RL, Sivakumaran H, Ranasinghe S, Rivera V,
410 Kondrashova O, Koufariotis LT, Du X, Driguez P, French JD, Waddell N, Duke
411 MG, Ittiprasert W, Mann VH, Brindley PJ, Jones MK, McManus DP. 2021.
412 CRISPR/Cas9-mediated genome editing of Schistosoma mansoni
413 acetylcholinesterase. FASEB J 35:e21205.
414 30. Shao H, Li X, Lok JB. 2017. Heritable genetic transformation of Strongyloides
415 stercoralis by microinjection of plasmid DNA constructs into the male
416 germline. Int J Parasitol 47:511-515.
417 31. Liu C, Grote A, Ghedin E, Unnasch TR. 2020. CRISPR-mediated Transfection of
418 Brugia malayi. PLoS Negl Trop Dis 14:e0008627.
419 32. Song C, Gallup JM, Day TA, Bartholomay LC, Kimber MJ. 2010. Development of
420 an in vivo RNAi protocol to investigate gene function in the filarial nematode,
421 Brugia malayi. PLoS Pathog 6:e1001239.
422 33. Misra S, Gupta J, Misra-Bhattacharya S. 2017. RNA interference mediated
423 knockdown of Brugia malayi UDP-Galactopyranose mutase severely affects
424 parasite viability, embryogenesis and in vivo development of infective larvae.
425 Parasit Vectors 10:34.
426 34. Iqbal S, Fosu-Nyarko J, Jones MG. 2016. Genomes of parasitic nematodes
427 (Meloidogyne hapla, Meloidogyne incognita, Ascaris suum and Brugia
428 malayi) have a reduced complement of small RNA interference pathway
429 genes: knockdown can reduce host infectivity of M. incognita. Funct Integr
430 Genomics 16:441-57.
431

432

Figure Legends

Figure 1. Evaluation of *Brugia malayi* L3 larvae sections under a transmission electron microscope showed that BmIL5Rbp is predominantly concentrated on the surface of the parasite (arrows), suggesting that BmIL5Rbp is expressed on the parasite's surface. The micrograph (A) shows worms coated with pre-immunized rabbit sera against BmIL5Rbp compared to the micrograph (B, C) using post-immunized rabbit sera identifying antibody localization on the worm's cuticle. Micrograph (C) is at higher magnification with Bar 500 nm.

Figure 2. Immunohistochemical staining localization with post-immunization rabbit sera to BmIL5Rbp and laser confocal microscopy on *Brugia malayi*. Worms were stained for BmIL5Rbp (red), nuclei (blue), and actin (green). Adult male worms (A, B), adult female worms (C, D), and infectious stage L3 worms (E, F) all express BmIL5Rbp on the surface of the cuticle. No BmIL5Rbp was seen internally in the worms, even dissected specimens. Control worms (B, D, F) had minimal red staining with pre-immunized rabbit sera to BmIL5Rbp.

Figure 3. (A) BmIL5Rbp mRNA expression in live *Brugia malayi* L3 larvae is inhibited using RNAi. RNAi-specific BmIL5Rbp dsRNA had a significant percent reduction to the internal control BmCPL dsRNA (33.1% versus 4.9% respectively, $p = 0.007$). A total of 450 worms were processed with an 85% survival rate in both groups. (B) RNAi inhibits BmIL5Rbp protein expression in

excretory/secretory products of live *Brugia malayi* L3 larvae compared to control worms (3.4 versus 8.2 pg/µL respectively, p = 0.034).

Figure 4. (A) RNAi can effectively reduce BmIL5Rbp on the surface of *Brugia malayi* L3 larvae. Intensity sum is the calculation of all red-stained BmIL5Rbp normalize to the total number of pixels (voxels) (Intensity Sum/Voxels) of all stained components of the worm. Pre-RNAi worms showed significant BmIL5Rbp staining to post-RNAi worms (2.125 Intensity Sum/Voxels compared to 1.146 Intensity Sum/Voxel respectively, p = 0.0025). (B) The supernatant (sups) from RNAi *Brugia malayi* L3 larvae contain less BmIL5Rbp in their excretory/secretory product compared to internal controls due to inhibition of protein expression (63.5% versus 85.1% respectively, p = 0.005).

Figure 1.

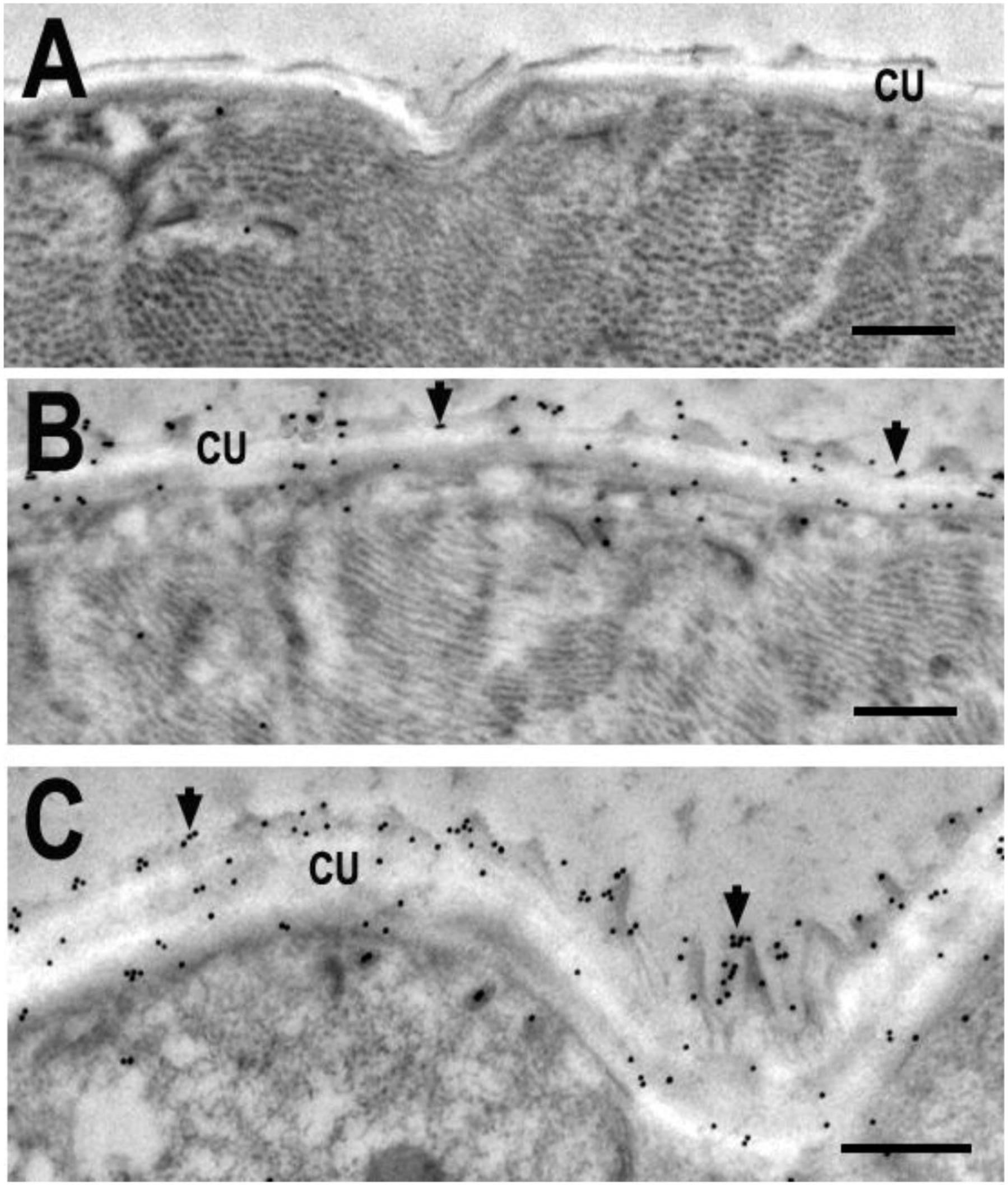

Pre-Immunization sera

Post Immunization sera

Figure 2.

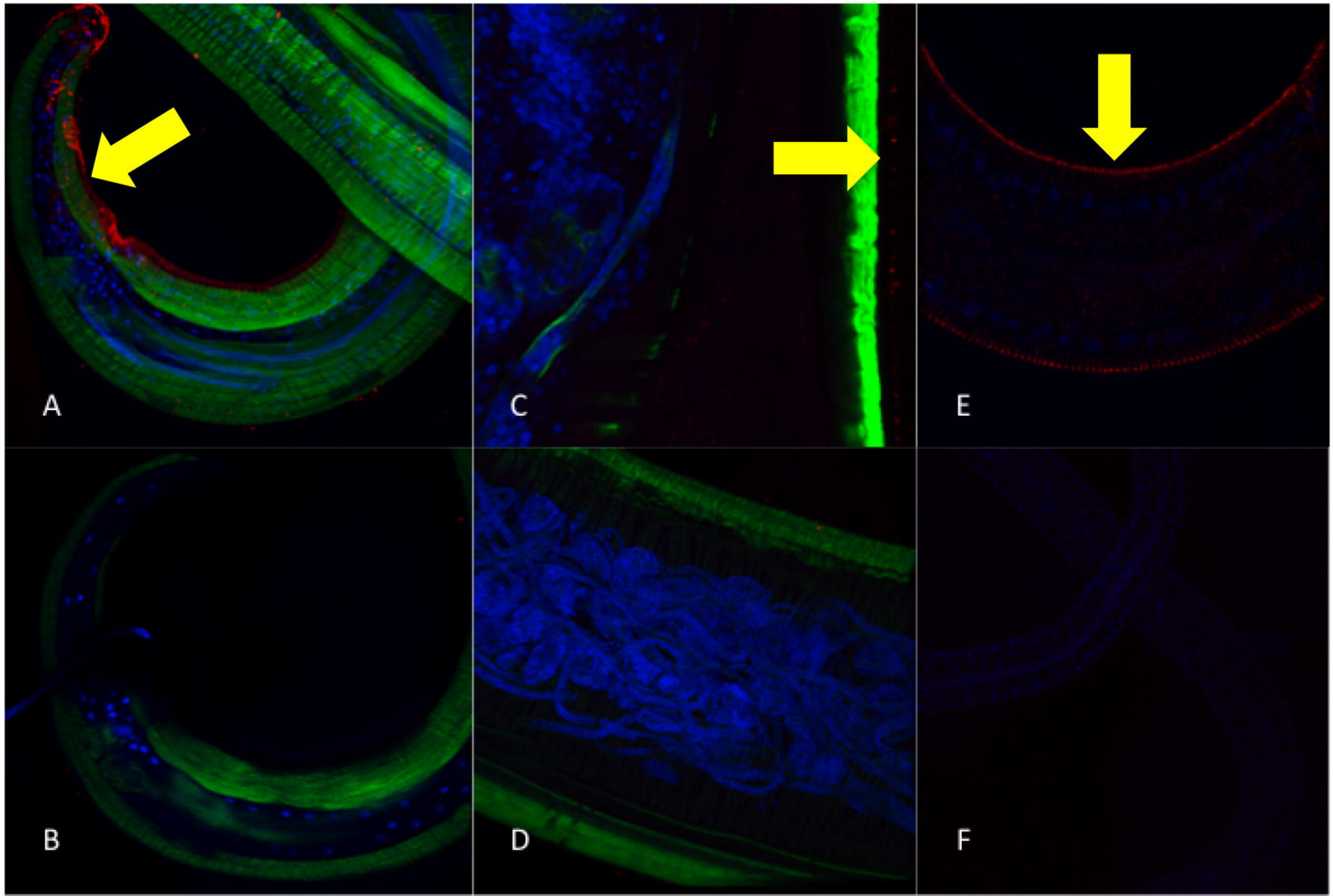

Figure 3.

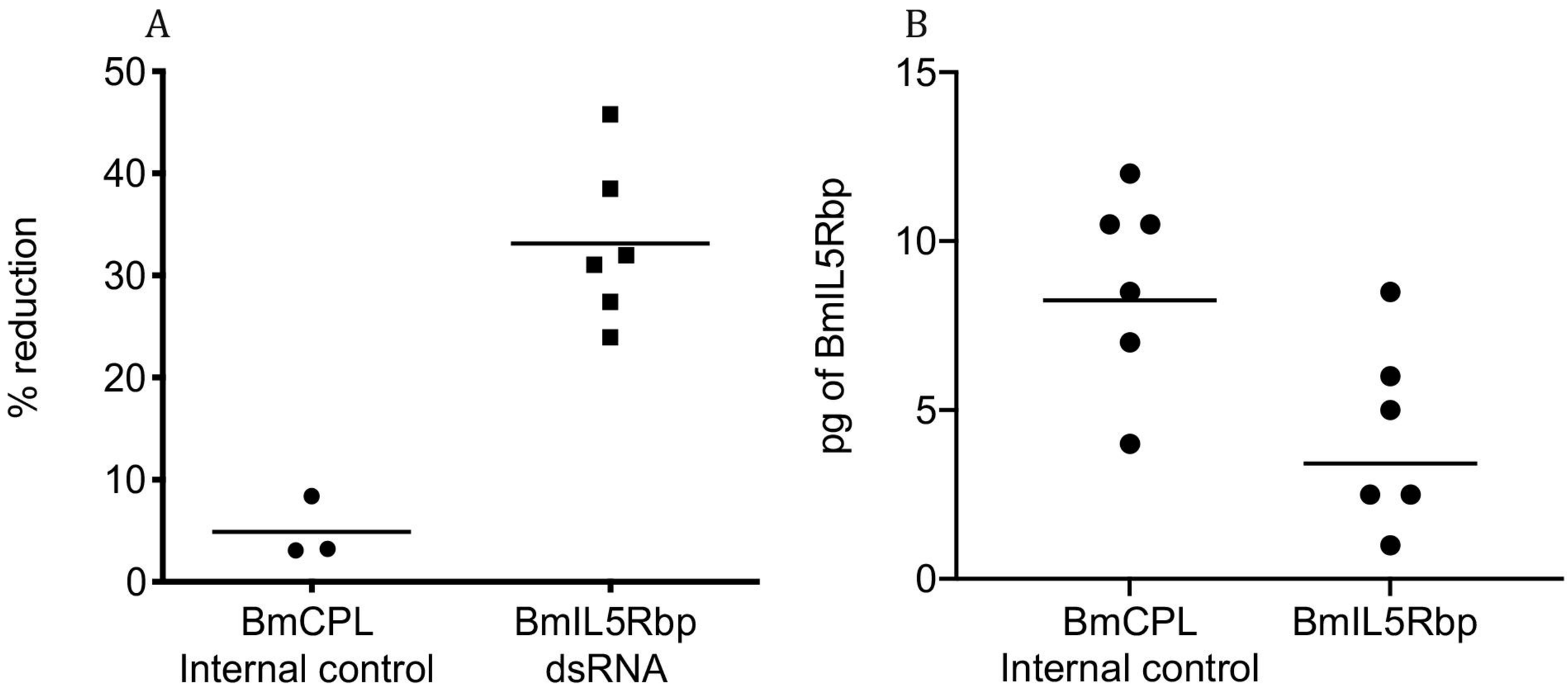
A
% reduction
50
40
30
20
10
0
BmCPL
Internal control
BmIL5Rbp
dsRNA
B
pg of BmIL5Rbp
15
10
5
0
BmCPL
Internal control
BmIL5Rbp

Figure 4.

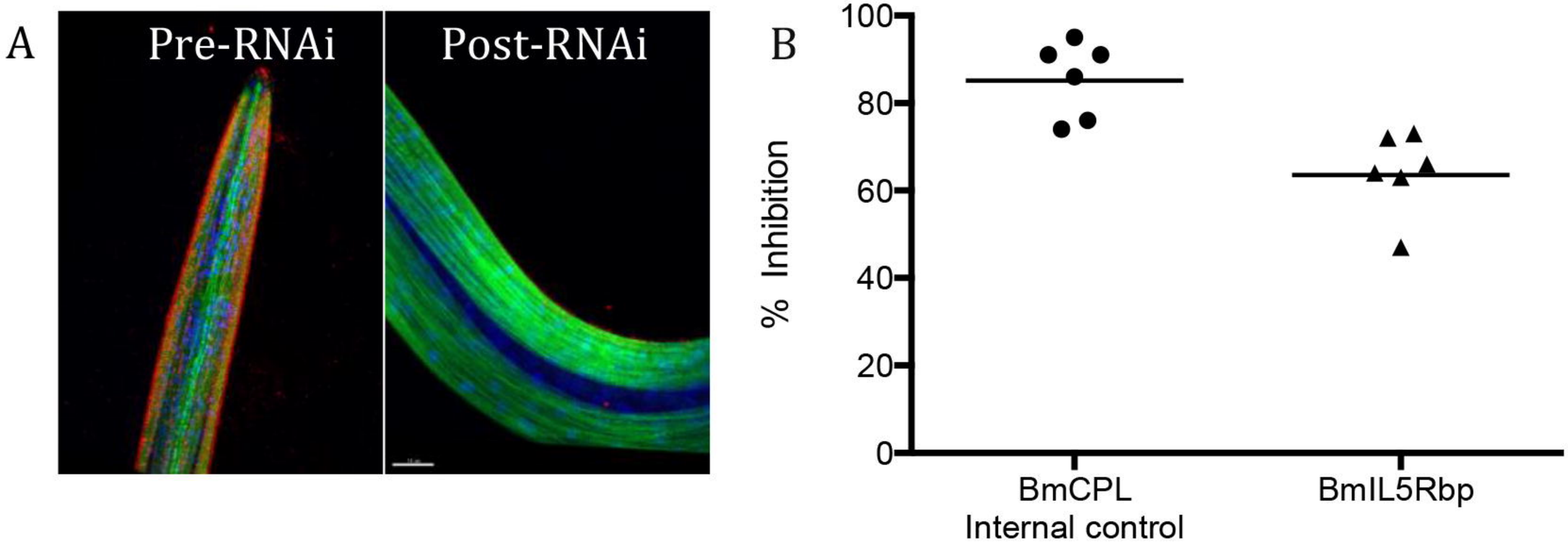
A
Pre-RNAi
Post-RNAi
B
% Inhibition
100
80
60
40
20
0
BmCPL
Internal control
BmIL5Rbp